UNIVERSITÀ DEGLI STUDI DEL PIEMONTE ORIENTALE

“AMEDEO AVOGADRO”

Master of science (MSc) in Food, Health and Environment

High-Fat Feeding Combined with Fructose Supplementation Promotes Body Weight Gain and Intramuscular Lipid Droplet Accumulation in In Vivo and In Vitro Models

Supervisor:

Prof.ssa Flavia Prodam

Candidate:

Nikoo Soleimani

Abstract

Sarcopenic obesity (SO) is a metabolic disorder marked by the simultaneous presence of excessive body fat and compromised skeletal muscle function, with diminished muscle mass and strength. Hypercaloric diets are widely acknowledged as significant factors in the development of obesity; however, their effects on skeletal muscle homeostasis and lipid metabolism are not fully elucidated. Specifically, the synergistic effects of elevated dietary fat and fructose intake on skeletal muscle remodeling and lipid accumulation necessitate further examination.

The current study aimed to assess the effects of chronic high-fat diet (HFD) intake, either independently or in conjunction with fructose supplementation (HFD+F), on skeletal muscle morphology, atrophic signaling, and lipid accumulation through integrated *in vivo* and *in vitro* methodologies. In the *in vivo* model, male C57BL/6J mice were administered *ad libitum* a normal diet (ND), a high-fat diet (HFD) comprising 45% of caloric intake from fat, or an HFD augmented with 30% fructose in their drinking water for a duration of 16 weeks. Body weight, adipose tissue depots, and skeletal muscle weights were evaluated. Myofiber cross-sectional area (CSA) and intramuscular lipid accumulation in tibialis anterior muscle were assessed using laminin and bodipy staining. Meanwhile, in *in vitro* experiments, differentiated C2C12 myotubes were exposed to palmitate (PA) with or without fructose (F) in order to further investigate the direct cellular effects of lipid and sugar excess.

Our results confirm an increase of body weight and white adipose tissue mass after prolonged exposure to HFD and HFD+F, indicating the development of an obese phenotype. Despite skeletal muscle weight and myofiber CSA did not change among the three groups, intramuscular lipid droplet accumulation was significantly increased in both HFD and HFD+F mice, indicating early metabolic remodeling within skeletal muscle. Notably, spleen and liver weights were elevated upon consumption of high caloric diet, which may indicate increased systemic inflammation and hepatic lipid accumulation. Additionally, *in vitro* tests showed that both fructose and palmitate caused a dose-dependent decrease in MyHC expression and myotube diameter, suggesting the activation of atrophic processes at the cellular level. The combined PA+F treatment resulted in the highest level of intracellular lipid accumulation, indicating additive effects on lipid storage, even though it did not worsen morphological atrophy when compared to individual treatments.

Overall, these results suggest that long-term exposure to a high-fat diet causes an early metabolic remodeling, impacting on intramuscular lipid droplet accumulation. On the other hand, we speculate that fructose supplementation is not pivotal in influencing directly muscle cell homeostasis, but it may worsen systemic metabolic disorders.

Introduction

2.1. Skeletal Muscle

Skeletal muscle is one of the most abundant tissues in the human body, containing approximately 40% of total body weight, and plays essential roles in everyday activities, including movement, posture, respiration, and metabolic regulation (1). It is composed of fascicles, which in turn encloses myofibers, that are long, cylindrical, and multinucleated cells containing myofibrils. Myofibrils are characterized by repeated contractile units called sarcomeres, which are pivotal for muscle contraction and force generation, through the interaction between actin and myosin filaments. This unique structural organization gives skeletal muscle its striated appearance under the microscope (2). Additionally, fascicles, myofibers, and the entire muscle are surrounded respectively by three connective tissue layers: the perimysium, endomysium, and epimysium. All of them provide structural support and allow for the passage of blood vessels and nerves (2).

Besides structural functions, skeletal muscle is also a key metabolic organ. It acts as a major site for glucose uptake and lipid oxidation, thus playing a central role in systemic energy homeostasis. It also serves as an amino acid reservoir during fasting or catabolic stress (3).

Furthermore, skeletal muscle is a highly plastic tissue, capable of adapting to various internal and external stimuli such as mechanical load, physical activity, nutrient availability, and hormonal signals. Its homeostasis is maintained by a dynamic balance between anabolic (protein synthesis) and catabolic (protein degradation) processes (3). When this homeostatic balance is disrupted by factors such as aging, physical inactivity, or pathological conditions, catabolic signaling predominates over anabolic pathways, driving skeletal muscle wasting and leading to a progressive decline in muscle mass and functional capacity, thereby predisposing to the development of muscle atrophy or sarcopenia (3–5).

2.2. Muscle Atrophy

Muscle atrophy is defined as a decrease in skeletal muscle mass resulting from an imbalance between protein synthesis and protein degradation, in which catabolic processes exceed anabolic signaling, ultimately leading to progressive loss of muscle tissue (3). It can arise from various conditions, including immobilization, aging, malnutrition, chronic inflammation, cancer, and metabolic disorders (3,6). A key feature of atrophy is the disruption of the balance between protein synthesis and degradation, with a shift toward increased proteolysis (6).

Two major proteolytic pathways are primarily responsible for muscle protein breakdown: the ubiquitin–proteasome system (UPS) and the autophagy–lysosome pathway (5). The UPS is activated through muscle-specific E3 ubiquitin ligases, such as atrogin-1 (Fbxo32) and muscle RING-finger protein-1 (MuRF1/Trim63), which tag muscle proteins for degradation via the proteasome (7). Increased expression of these ligases has been reported in several rodent models of muscle atrophy, including denervation, disuse (hindlimb unloading), and fasting, as well as in muscle biopsies from patients affected by muscle wasting conditions such as sarcopenia and cancer cachexia (7). The activation of these proteolytic pathways contributes to the progressive loss of muscle proteins and cellular components, leading to a reduction in muscle mass and contractile capacity. As a consequence, muscle atrophy impairs muscle strength and physical performance, ultimately compromising mobility and metabolic homeostasis (3).

In addition to these proteolytic systems, oxidative stress and chronic inflammation play significant roles in muscle atrophy. Elevated levels of pro-inflammatory cytokines, such as interleukin-6 (IL-6), and an increase in reactive oxygen species (ROS) can directly impair protein synthesis and activate proteolytic pathways (6). These molecular changes synergistically contribute in reducing muscle fiber size, impairing contractile function, and increasing susceptibility to fatigue (8).

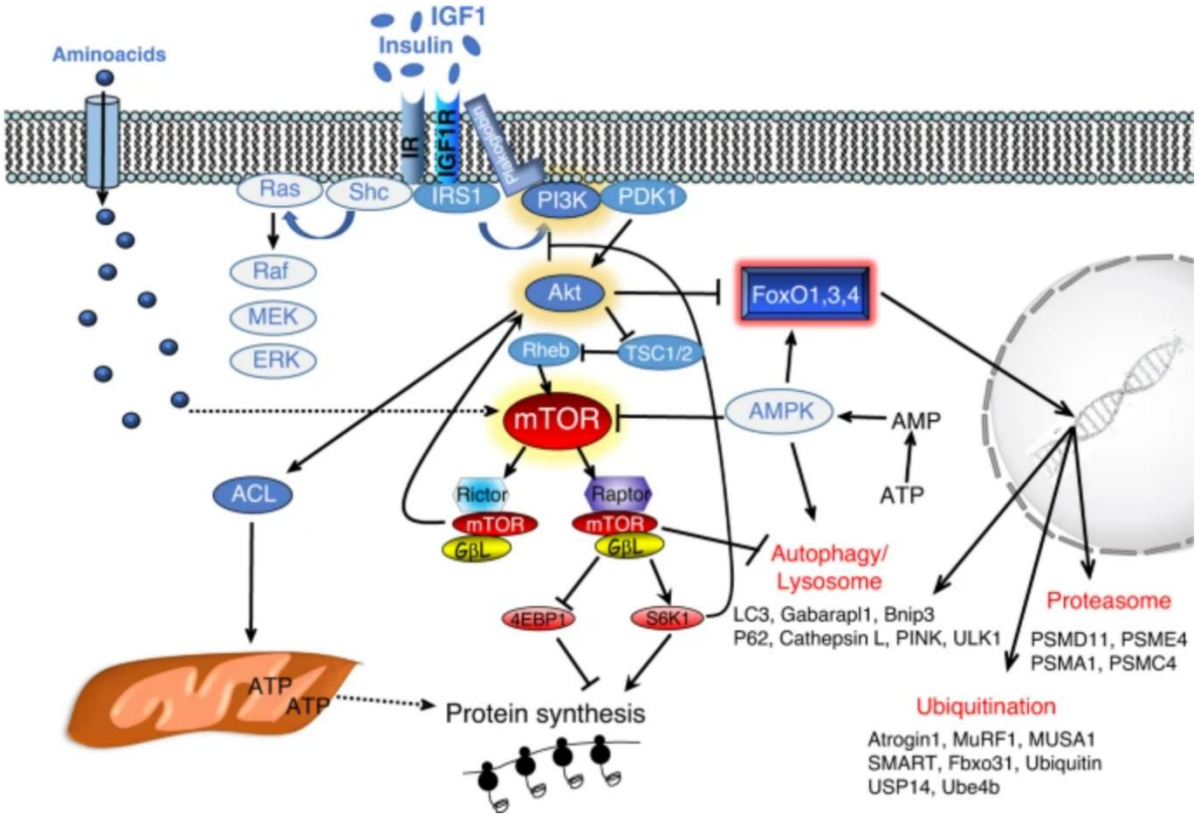

Figure 1. Major proteolytic pathways and signaling cascades involved in skeletal muscle atrophy. (Sartori, R., Romanello, V., & Sandri, M. (2021). Mechanisms of muscle atrophy and hypertrophy: implications in health and disease. *Nature Communications*, 12(1), 330.)

Chronic consumption of hypercaloric, Western-style diets are widely demonstrated to promote systemic metabolic dysfunction, characterized by increased adiposity, insulin resistance, and chronic low-grade inflammation, conditions that collectively contributes to muscle atrophy by shifting the balance toward catabolic pathways, ultimately exacerbating functional decline despite increased body weight (9). In this context, excess nutrient availability coexists with a paradoxical loss of muscle mass and function, a condition referred to as sarcopenic obesity (10).

2.3. Sarcopenic Obesity

Sarcopenic obesity (SO) is a condition characterized by the coexistence of excessive fat accumulation and a simultaneous reduction in skeletal muscle mass and strength. This combination worsens the functional and metabolic consequences of both obesity and sarcopenia, and is associated with a higher risk of disability, insulin resistance, type 2 diabetes, cardiovascular diseases, and overall mortality compared to either condition alone (11). Clinically, SO is identified when an individual has a high body fat percentage together with reduced muscle mass and low muscle strength or poor performances (12). This condition

requires combined intervention strategies, including resistance exercise to stimulate muscle protein synthesis, aerobic exercise to reduce fat mass, and dietary modifications that ensure adequate protein intake along with controlled energy intake (8). Early recognition and targeted treatment are essential to prevent further decline in physical function and reduce metabolic complications. Several mechanisms contribute to the development of SO, including aging, sedentary lifestyle, chronic inflammation, mitochondrial dysfunction, hormonal changes (such as declines in testosterone, growth hormone, or estrogen), and nutritional imbalance.

In individuals with SO, adipose tissue could infiltrate within muscle fibers, as lipid droplets, whose role is to store fat in the form of triglycerides when there is an excess of fatty acids in the body. Under normal condition, lipid droplets have a key role both in keeping extra fatty acids in a safe form, releasing them when the body needs energy, and recycling them through autophagy (13). However, in particular conditions, especially in obese people, when lipid accumulation is too high, this protective system becomes overwhelmed and fat accumulates not only in adipose tissue but also in other tissues and organs, including liver and skeletal muscle (14). This abnormal build-up of fat can interfere with normal muscle function and contribute to muscle weakness. Excess lipid droplets not only impact on the production of pro-inflammatory cytokines, such as tumor necrosis factor (TNF-α) and IL-6, but also on adipokines level dysregulation, like leptin and adiponectin, triggering systemic metabolic complications, including in skeletal muscle tissue (15,16).

As a consequence, as confirmed by Wannamethee and Batsis studies, muscle strength is impaired and physical activity is reduced, favoring additional fat accumulation and muscle wasting (11,15). For these reasons, high-fat and high-sugar diets have been widely demonstrated to be pivotal in the onset of SO and the related health complications (12,15).

2.4. High-Fat Diet

A high-fat diet (HFD), generally defined as providing approximately 30–60% of total caloric intake from fat, represents a key experimental approach for studying metabolic disorders associated with nutrient excess.

Originally introduced in experimental research during the mid-20th century, HFD models have consistently demonstrated the ability to induce metabolic disturbances such as hyperglycemia, insulin resistance, and chronic low-grade inflammation (17). A defining characteristic of HFD consumption is excessive lipid accumulation, which strongly contributes to the development of obesity and related metabolic complications (18,19).

This effect is primarily driven by sustained positive energy balance and alterations in macro- and micronutrient intake, ultimately leading to an expansion of adipose tissue mass (17,20,21). Consequently, HFD is widely recognized as one of the most effective dietary models for inducing obesity in both humans and animal studies. The physiological consequences of HFD exposure are influenced by both the duration of dietary intervention and the total fat content consumed (22). The lipotoxic environment generated by prolonged HFD exposure promotes metabolic dysfunction through several mechanisms. Among these, mitochondrial impairment and increased oxidative stress play a central role, contributing to endoplasmic reticulum stress, apoptosis, and enhanced protein degradation pathways (23). Furthermore, chronic HFD consumption is associated with the development of hyperinsulinemia and impaired glucose tolerance, reflecting reduced insulin sensitivity — hallmark features of obesity-related metabolic dysfunction (21).

Moreover, the increased use of fructose in modern diets, mainly through sucrose and high-fructose corn syrup (HFCS), has been strongly linked to the global rise of obesity and metabolic diseases. Fructose is a monosaccharide commonly found in fruits, honey, and, more importantly, as part of added sugars such as sucrose and high-fructose corn syrup (HFCS). Unlike glucose, fructose is mainly metabolized in the liver, where it enters glycolysis independently of insulin by being converted into fructose-1-phosphate via fructokinase (ketohexokinase) (24). This bypass of the key glycolytic enzyme phosphofructokinase results in uncontrolled and rapid conversion of fructose into intermediates of lipogenesis, promoting the synthesis of triglycerides and leading to de novo lipogenesis (25).

High intake of fructose has been associated with increased hepatic fat accumulation, elevated triglyceride levels in the blood, and insulin resistance (26). In addition, fructose metabolism leads to the production of uric acid, which can contribute to oxidative stress and inflammation (27).Chronic fructose consumption has been shown to trigger metabolic dysfunction including dyslipidemia, hepatic steatosis, hypertension, and obesity.

Recent studies have also highlighted the negative role of fructose on skeletal muscle tissue. Excessive fructose intake can impair insulin signaling in muscle cells, decreasing insulin secretion or leptin production, two key hormones involved in appetite regulation and energy balance (24), may leading to increased energy consumption and weight gain (26).

Experimental studies and clinical evidence have demonstrated that chronic consumption of fructose promotes fat deposition in the liver and visceral adipose tissue, contributing to obesity (28). This effect is largely due to fructose-driven hepatic de novo lipogenesis, which increases triglyceride synthesis and fat accumulation (29). Moreover, fructose consumption has been shown to increase circulating triglycerides and very low-density lipoprotein (VLDL), both of which are associated with obesity-related metabolic disorders (25).

Preclinical studies in animal models have shown that high-fructose feeding increases adiposity, promotes insulin resistance, and disrupts lipid metabolism, even in the absence of a proportional rise in total caloric intake(28,29). In humans, excessive consumption of sugar-sweetened beverages containing high-fructose corn syrup (HFCS) has consistently been associated with an increased risk of obesity and metabolic syndrome(24–26).

Aim of the project

Given this, high-fructose diets are widely regarded as a major dietary contributor to the onset and progression of obesity. Despite this evidence, the role of fructose in skeletal muscle, particularly in the context of a high-fat, high-fructose dietary regimen, remains insufficiently characterized. Therefore, the primary objective of this project was to investigate the impact of a high-fat, high-fructose diet on skeletal muscle homeostasis, feeding three groups of mice with different dietary regimens: standard diet (SD), high-fat diet (HFD), and high-fat diet supplemented with fructose (HFD+F). Furthermore, to mimic them *in vitro* C2C12 myotubes, the widely used cell model to mimic skeletal muscle, were treated with palmitate, the most abundant saturated fatty acid found in circulation upon consumption of diet rich in fat, with or without fructose addition.

Materials and Methods

3.1 *In Vivo* Experiments

All animal procedures were conducted in accordance with the European Community Directive 2010/63/EU for the protection of animals used for scientific purposes and were approved by the Institutional Animal Care and Use Committee of the University of Piemonte Orientale (authorization n. 893/2023-PR). Male C57BL/6J mice (8–9 weeks old) were obtained from Charles River Laboratories (Italy) and housed in groups of four to five per cage under controlled environmental conditions (22 ± 1 °C, 55% humidity, 12-hour light/dark cycle). Animals had free access to food and water throughout the experimental period.

3.1.1 Experimental Plan

After a one-week acclimatization period on a normal chow diet, mice were randomly assigned to three dietary conditions: a normal diet (ND), a high-fat diet (HFD), or a high-fat diet supplemented with fructose in the drinking water (HFD+F). The HFD provided 45% of total calories from fat, while animals in the HFD+F group received the same diet together with a 30% (w/v) fructose solution dissolved in their drinking water. The intervention period lasted 16 weeks. Body weight and food intake were recorded weekly, and drinking volume was measured every two days to monitor fructose consumption. All animals were observed daily to ensure proper health conditions and to identify any signs of distress or abnormal behavior.

At the end of the experimental period, mice were anesthetized with 4% isoflurane, and euthanized by cervical dislocation in accordance with institutional ethical guidelines. Skeletal muscles from the hind limbs, including gastrocnemius (GA), tibialis anterior (TA), and quadriceps (QUAD), were rapidly dissected, cleaned of surrounding tissues, weighed, and either snap-frozen in liquid nitrogen for molecular analyses or embedded in optimal cutting temperature (OCT) compound for cryosectioning and histological evaluation. All collected samples were stored at −80 °C until further use. In addition, epididymal and subcutaneous adipose tissues were harvested and weighed to assess systemic metabolic adaptations associated with the different dietary interventions.

3.2 *IN VITRO*

3.2.1 Cell Culture and Myotube Analysis

C2C12 murine myoblasts (ECACC, UK) were used as the *in vitro* model for skeletal muscle differentiation. Cells were cultured in Dulbecco's Modified Eagle Medium (DMEM, Gibco, Thermo Fisher Scientific, USA) containing 10% fetal bovine serum (FBS), 1% penicillin–streptomycin, and 1% amphotericin B. Cultures were maintained at 37°C in a humidified atmosphere with 5% CO_2 and 95% air. The medium was changed every two days until the cells reached approximately 80–90% confluence.

To induce differentiation, the growth medium was replaced with differentiation medium (DM), consisting of DMEM supplemented with 2% horse serum (HS). Myoblasts were allowed to fuse and form multinucleated myotubes over a period of 5 to 7 days, during which the differentiation medium was renewed every 48 hours. The degree of differentiation was confirmed microscopically by the appearance of elongated, multinucleated fibers typical of mature myotubes.

Once full differentiation was achieved, myotubes were exposed to metabolic stressors to mimic conditions associated with dietary fructose intake and lipid overload. Treatments included fructose (100, 500 μM) and/or palmitate (500 μM) for 24 hours in serum-free DMEM or in DM 2% HS, depending on the

experimental setup. These concentrations were chosen based on previous studies showing physiological relevance in reproducing the effects of high-fructose and high-fat exposure *in vitro*. Control cells were maintained under the same conditions and treated with the respective vehicle (0.1% ethanol).

For every experiment were measured at least 10 myotubes diameter for each field, five different fields for each replicate, and three technical replicates for each used treatment. Myotubes diameters were measured with JMicroVision software.3.2.2 Western Blot Analysis.

After the treatment period, C2C12 myotubes were gently washed twice with ice-cold phosphate-buffered saline (PBS) to remove residual medium and detached metabolites. The cells were then lysed in an ice-cold lysis buffer containing 1% Triton X-100, 0.1% sodium deoxycholate, 0.1% SDS, 1 mM EDTA, 1 mM EGTA, 50 mM NaF, 160 mM NaCl, and 20 mM Tris-HCl (pH 7.4), freshly supplemented with a protease and phosphatase inhibitor cocktail (Roche). Lysates were stirred for 15 minutes at 4°C and centrifuged at 15,000 × g for 15 min at 4° C. The concentration of proteins was determined by BCA protein assay kit. Proteins were resuspended in sample buffer containing 2% SDS, 150 mM dithiothreitol (DTT), and 0.01% bromophenol blue, and 20 µg protein/lane were separated by 10 or 15% SDS-PAGE and transferred to PVDF.

Membranes were saturated with 4% BSA, probed with the primary antibodies overnight at 4 °C, washed with tris-buffered saline (TBS) 0.1% Tween, incubated with the appropriate secondary antibody for 1 hour at room temperature, visualized with Western Lightning Chemiluminescence Reagent Plus (Perkin Elmer Life and Analytical Sciences), acquired with ChemiDoc Touch (Bio-Rad), and analyzed with ImageLab (Bio-Rad).

All experiments were conducted in at least three biological replicates to ensure reproducibility, and results were expressed as mean ± standard error of the mean (SEM).

3.2.3 Bodipy Staining

To visualize and quantify lipid droplet (LD) accumulation in C2C12 myotubes, a fluorescent staining protocol using Bodipy 493/503 (Thermo Fisher Scientific, USA) was performed. After the treatment period, cells were gently washed twice with phosphate-buffered saline (PBS) to remove culture medium and fixed with 4% paraformaldehyde (PFA) for 10 minutes at room temperature. Following fixation, cells were rinsed again with PBS and incubated with Bodipy 493/503 working solution (1 µg/mL in PBS) for 30 minutes in the dark to allow selective staining of neutral lipids.

After staining, nuclei were counterstained with 4’,6-diamidino-2-phenylindole (DAPI; 1 µg/mL, Sigma-Aldrich) for 5 minutes to facilitate visualization of cell morphology. The samples were then mounted with an antifade mounting medium and examined under a fluorescence microscope (EVOS™ XL Core Imaging System, Thermo Fisher Scientific) equipped with FITC and DAPI filters.

Images were captured from at least five randomly selected fields per well using identical exposure settings for all experimental conditions. Lipid droplet number and fluorescence intensity were quantified using ImageJ (NIH, USA). Data were expressed as the mean Bodipy fluorescence intensity per myotube or per unit area, normalized to the control group.

3.3 Ex Vivo Analyses

3.3.1 Cross-Sectional Area (CSA) Immunofluorescence

Frozen muscle samples (gastrocnemius) were cut into 7 µm-thick sections at the mid-belly region using a cryostat (Leica CM1950). Sections were mounted on glass slides, air-dried, and fixed with 4% paraformaldehyde (PFA) for 10 minutes at room temperature. After washing in phosphate-buffered saline (PBS), sections were permeabilized with 0.2% Triton X-100 for 5 minutes and blocked with 4% bovine serum albumin (BSA) for 30 minutes to reduce non-specific binding.

For the identification of muscle fiber borders, samples were incubated overnight at 4°C with an anti-laminin primary antibody (1:400, Sigma-Aldrich). The next day, slides were washed and incubated with Alexa Fluor-conjugated secondary antibodies (1:1000, Thermo Fisher Scientific) for 45 minutes in the dark. Nuclei were counterstained with DAPI (1 µg/mL) for 5 minutes.

Images were acquired using a Leica TCS SP8 confocal microscope. Cross-sectional area (CSA) of at least 200 fibers per muscle was measured using ImageJ software (NIH, USA). Data were expressed as mean fiber area (μm^2) ± standard error of the mean (SEM).

3.3.2 Bodipy Staining of Muscle Tissue

To evaluate lipid droplet (LD) accumulation in skeletal muscle, 7 µm cryosections were fixed in 4% PFA for 10 minutes, washed with PBS, and incubated with Bodipy 493/503 (1:5000 dilution in PBS) for 30 minutes in the dark. Nuclei were counterstained with DAPI (1 µg/mL) for 10 minutes. Slides were mounted with an antifade medium and imaged under a fluorescence microscope (EVOS™ XL Core Imaging System).

For each muscle sample, at least five random fields were analyzed. The Bodipy-positive area was quantified using ImageJ and expressed as a percentage of total tissue area. All analyses were performed blindly to avoid observer bias.

3.4 Data Analysis

All data were analyzed using GraphPad Prism 8.0 software (GraphPad Software, USA). Before statistical evaluation, datasets were examined for outliers using the interquartile range (IQR) method, and any extreme values were excluded if justified by technical error.

Results are presented as mean ± standard error of the mean (SEM). Comparisons between two groups were performed using the unpaired Student's *t*-test. When more than two groups were compared, a one-way analysis of variance (ANOVA) was applied, followed by Tukey's post-hoc test for multiple comparisons.

A value of $p < 0.05$ was considered statistically significant. All experiments were performed at least in triplicate to ensure reproducibility.

Graphical data were generated using GraphPad Prism, and representative images were prepared with Adobe Illustrator (Adobe Systems, USA) for figure assembly.

Results

4.1 HFD both alone and in combination with fructose increased mice mass without altering muscle weights

To investigate the effects of free fatty acids and fructose in an animal model, mice were purchased at 3 weeks of age and maintained on a normal diet (ND) for six weeks to allow proper acclimatization. At 9 weeks of age, animals were randomly assigned to three dietary groups, ND, High-Fat Diet (HFD), and High-Fat Diet supplemented with fructose (HFD+F). Mice were kept on these regimens for 16 weeks, until 25 weeks of age.

As shown in Figure 2A, body weight was monitored every four weeks to assess the progression of weight gain across dietary groups. A significant increase in body weight was observed in mice fed the HFD, with or without fructose supplementation, when compared with ND controls. Notably, mice receiving fructose in addition to the high-fat diet displayed a marked increase in body weight already during the first month of treatment. In contrast, mice fed only the HFD showed a significant increase starting from the second recorded time point. These differences persisted throughout the entire experimental period and remained evident at the endpoint. Such sustained weight gain may partially explain the reduced muscle strength and impaired functional performance observed in these groups (data not shown).

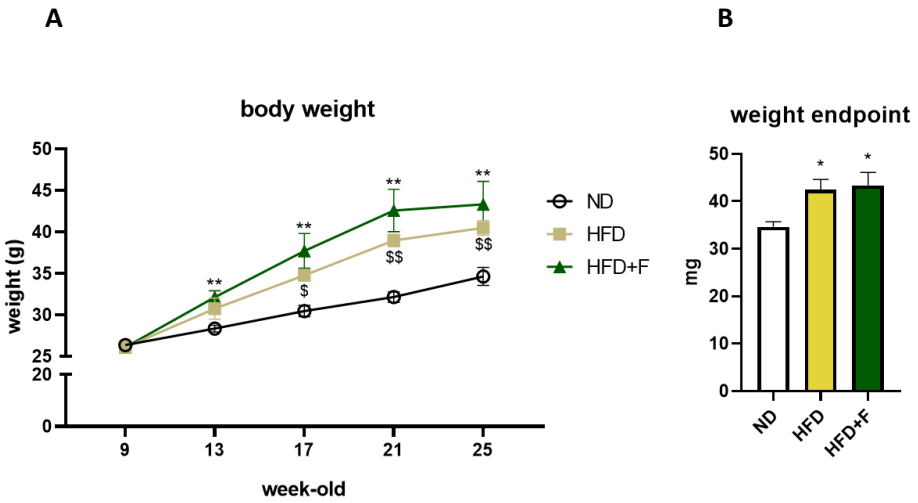

Figure 2. High-fat diet, with or without fructose supplementation, leads to a progressive increase in body weight over the 16-week feeding period (A). Mice were weighed every four weeks starting from 9 weeks of age. A similar pattern is observed in the endpoint weight graph (B). Data are expressed as mean ± standard error of the mean (SEM). Statistical significance is indicated as **p < 0.01 and *p < 0.05. Analyses were performed using Student's *t*-test and two-way ANOVA.

Given the substantial increase in body weight observed in HFD and HFD+F mice, we evaluated whether this weight gain was accompanied by a disproportionate fat accumulation in adipose tissue at the expense of muscle mass, a hallmark of sarcopenic obesity. To this aim, both adipose depots and skeletal muscles were weighed and stored at sacrifice.

As shown in Figure 3, epididymal fat (eFAT, Figure 3A) and subcutaneous fat (sFAT, Figure 3B) displayed similar patterns, both fats resulted significantly increased in mice fed with HFD or HFD+F compared with ND ones. Notably, animals subjected to either dietary treatment exhibited approximately a two-fold

increase in eFAT and sFAT, corresponding to an average difference of nearly 15 mg/mm relative to ND. However, fructose was not sufficient in further impacting its accumulation, thus the difference between HFD and HFD+F mice is minimal, amounting to roughly 5 mg/mm in both fat depots. On the other hand, no statistically significant differences were detected across the dietary groups in brown adipose tissue graph (Figure 3C), in which only a slight increase was observed in HFD+F group.

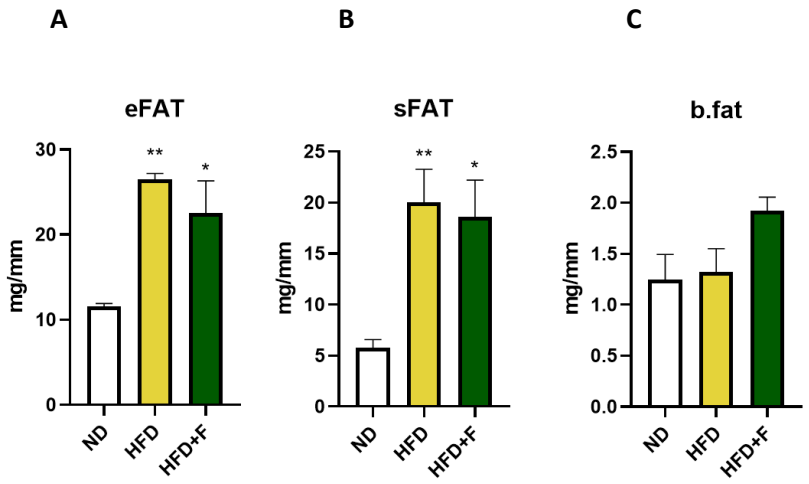

Figure 3. High-fat diet, with or without fructose supplementation, induces a significant increase in epididymal (A) and subcutaneous (B) fat compared with normal diet. No statistically significant differences were observed in brown adipose tissue among ND, HFD, and HFD+F groups (C). Data are presented as mean ± standard error of the mean (SEM). Statistical significance was set at $^{**}p < 0.01$. Analyses were performed using Student's *t*-test and ANOVA.

Although a substantial increase in fat mass upon HFD and HFD+F consumption was appreciated, this was not accompanied by a reduction in skeletal muscle mass. As shown in Figure 4A–C, the weights of the major hindlimb muscles, including the gastrocnemius (GA), tibialis anterior (TA), and quadriceps (QUAD), did not differ among the dietary groups. All muscle weights displayed a similar pattern, with no detectable shifts between ND, HFD, and HFD+F mice. These findings indicate that, despite the clear diet-induced obesity, skeletal muscle mass remained unaffected by the dietary interventions.

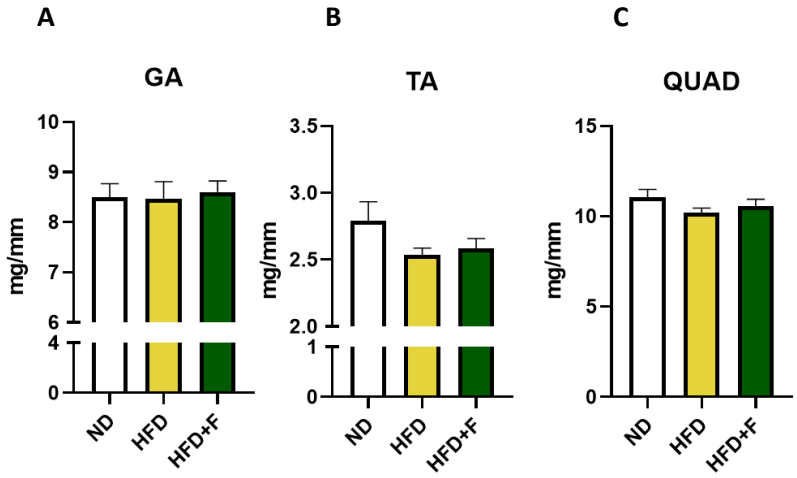

Figure 4. No significant differences in muscle weight were observed among dietary groups in the gastrocnemius (GA, A), tibialis anterior (TA, B), and quadriceps (QUAD, C). Data are presented as mean ± standard error of the mean (SEM). Statistical analysis was performed using Student's *t*-test and ANOVA.

Interestingly, we extended our analysis to other organs to evaluate potential systemic effects and notably, fructose supplementation alone was sufficient to significantly increase spleen weight compared not only with ND but also with HFD (Figure 5A). This finding suggests that fructose may directly contribute to systemic inflammation and organ-specific alterations, independent of dietary fat content. In addition, liver weight was also elevated in the HFD+F group (Figure 5B), supporting the possibility that fructose intake promotes hepatic lipid accumulation and may contribute to the development of steatosis.

Together, these results highlight the broader systemic consequences of excessive fructose consumption, demonstrating its capacity to exacerbate inflammation and induce pathological remodeling in peripheral organs beyond skeletal muscle.

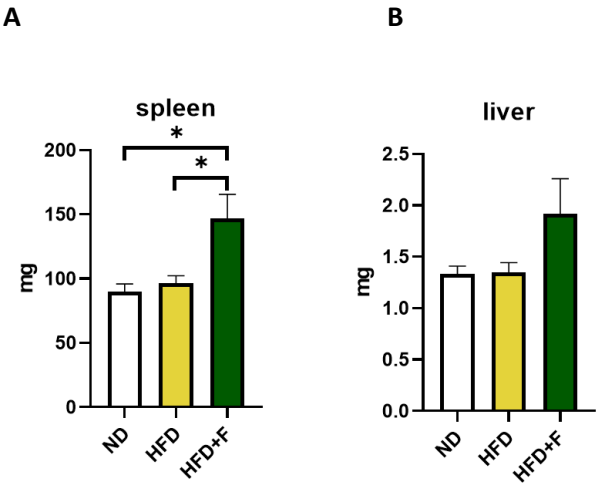

Figure 5. HFD+F increases spleen (A) and liver (B) weight compared with control groups. Data are presented as mean ± standard error of the mean (SEM). Statistical analysis was performed using ANOVA.

4.1.1 Consumption of HFD with or without fructose supplementation did not impact myofiber size, but promoted intramuscular lipid accumulation

Tibialis anterior muscles (TA) were used to investigate myofiber morphology through anti-laminin staining, useful to quantify the area of each fiber. Laminin staining outlines the structural integrity of individual fibers and, together with DAPI nuclear staining, shows that the overall organization and histological architecture of the muscle remain preserved across all dietary groups. As is depicted by the representative images and the graph, no shifts were appreciated in myofiber size, coherently with the absence of muscle mass differences.

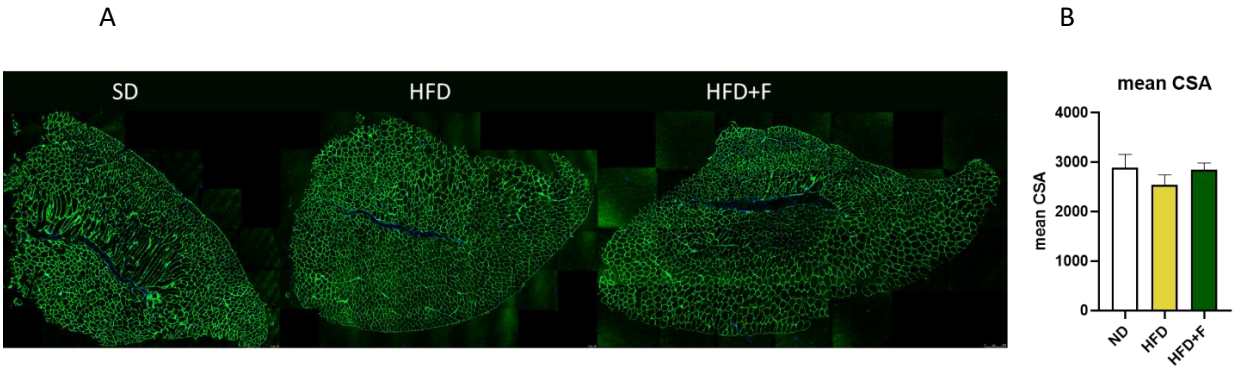

Figure 6. Analysis of myofiber cross-sectional area (CSA) in tibialis anterior muscle.

(A) Representative laminin-stained cross-sections of tibialis anterior (TA) muscles from mice fed normal diet (ND), high-fat diet (HFD), or high-fat diet supplemented with fructose (HFD+F). Laminin staining outlines the sarcolemma of individual muscle fibers, allowing visualization of muscle architecture and accurate identification of myofiber boundaries. **(B)** Quantification of the mean cross-sectional area (CSA) of TA muscle fibers in the different dietary groups. No significant differences in myofiber size were observed among ND, HFD, and HFD+F groups. Data are presented as mean ± SEM.

These findings paved the way to investigate whether the accumulation of intramuscular lipid droplets might account for the apparent lack of atrophy in hindlimb muscles. Representative TA cross-sections from ND, HFD, and HFD+F mice reveal clear differences in intramuscular lipid accumulation across dietary conditions. Bodipy staining in combination with anti-laminin antibody was performed in order to stain both lipid droplets and the myofibers. The percentage of bodipy positive (bodipy+) fibers relative to total myofibers was quantified to detect variations among the three experimental groups. In mice fed a normal diet, bodipy staining appears minimal, with only scattered lipid droplets detectable within muscle fibers (FIG 7). In contrast, as shown in Figure 7, both HFD and HFD+F muscles exhibited a significantly higher percentage of bodipy+ fibers relative to total myofibers compared with ND. No significant difference between HFD and HFD+F were evident, indicating that fructose supplementation did not further enhance lipid-positive fiber prevalence beyond the effect of HFD alone (FIG 7).

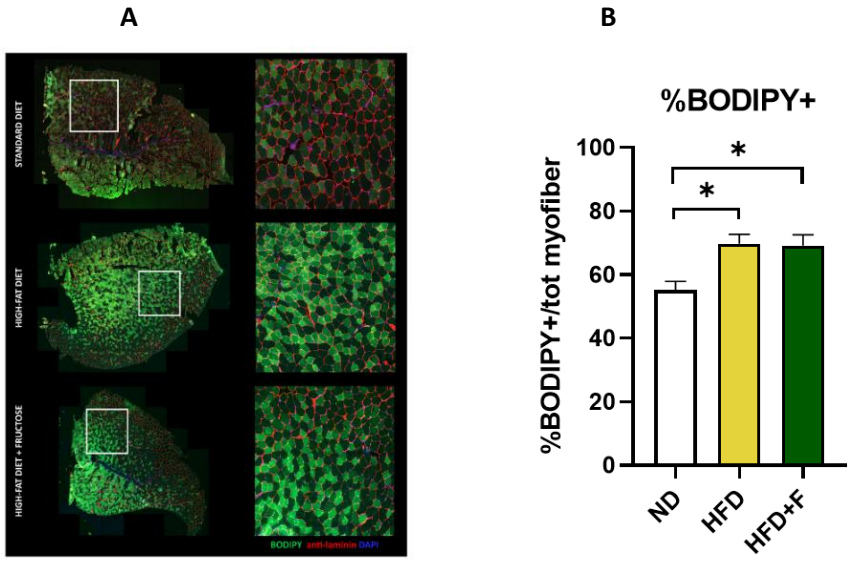

Figure 7. Increase of ipid droplet accumulation HFD-dependent (A) Representative immunofluorescence images of tibialis anterior (TA) muscle sections from mice fed normal diet (ND), high-fat diet (HFD), or high-fat diet supplemented with fructose (HFD+F). Sections were stained with BODIPY (lipid droplets, green), anti-laminin (myofiber boundaries, red), and DAPI (nuclei, blue). Whole-section images and higher-magnification views are shown. Increased BODIPY staining is visible in HFD and HFD+F muscles compared with ND, indicating greater intramuscular lipid accumulation. **(B)** Quantification of intramuscular lipid accumulation expressed as the percentage of BODIPY-positive myofibers over the total number of myofibers in TA muscle. Both HFD and HFD+F groups show a significant increase in BODIPY-positive myofibers compared with ND. Data are presented as mean ± SEM.

Despite the pronounced increase in lipid accumulation in HFD and HFD+F mice, the general morphology of the fibers does not appear altered, confirming that CSA (FIG 6B), either the bodipy+ and bodipy- were not altered by dietary regimens (FIG 8).

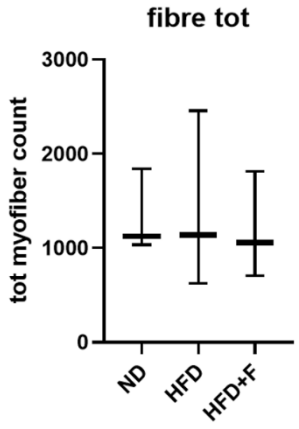

Figure 8. Absence of total myofiber count variation. Total number of myofibers quantified in tibialis anterior (TA) muscle sections from mice fed normal diet (ND), high-fat diet (HFD), or high-fat diet supplemented with fructose (HFD+F). No significant differences in total myofiber number were observed among the experimental groups. Data are presented as mean ± SEM.

Together, these results indicate that despite increased intramuscular lipid deposition in HFD and HFD+F mice, lipid-rich and lipid-poor fiber size remained unchanged.

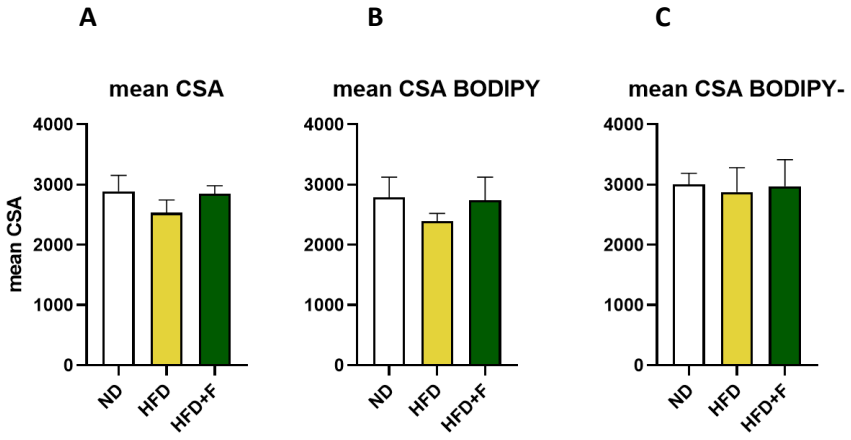

Figure 9. *Analysis of myofiber cross-sectional area (CSA) in TA muscle under different dietary conditions.* Mean CSA (A), mean CSA of BODIPY^{+} fibers (B), and mean CSA of BODIPY^{-} fibers (C) were quantified in ND, HFD, and HFD+F mice. No significant differences were detected in overall fiber size or in the CSA of lipid-containing versus non–lipid-containing myofibers among the three groups, indicating that neither HFD nor HFD+F induced measurable fiber atrophy at the morphological level. Data are expressed as mean ± S.E.M.

4.2 Palmitate and Fructose Treatments Decrease C2C12 Myotube Diameter and Their Combination Exacerbates Atrophic Responses

To evaluate whether nutrient overload contributes to skeletal muscle atrophy *in vitro*, differentiated C2C12 myotubes were used to mimic skeletal muscle, as widely demonstrated in literature. Myotubes were exposed for 24 hours to increasing concentrations of palmitate (PA100 µM, PA250 µM, PA500 µM) or fructose (F100 µM, F500 µM). Treatments were performed in serum-free DMEM, and myotube diameters were measured to understand whether treatments could induce hypertrophy or atrophy.

As shown in panels A–D, both palmitate and fructose induced a dose-dependent decrease in myotube diameter. Palmitate significantly reduced myotube width at higher concentrations, with the most pronounced effect observed at 500 µM. Similarly, fructose exposure led to a marked reduction in myotube diameter, particularly at the 500 µM concentration.

A

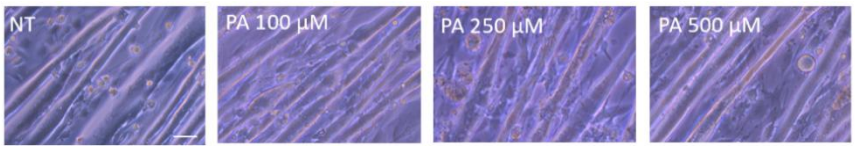

B

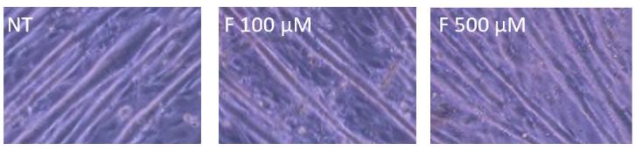

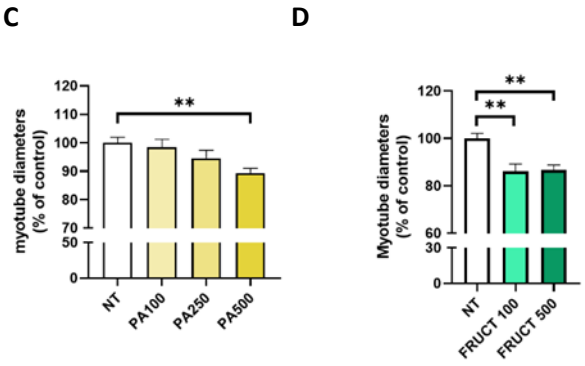

Figure 10. Palmitate and fructose reduce C2C12 myotube diameter in a dose-dependent manner, and their combination further exacerbates this effect. (A–B) Representative bright-field images of myotubes treated with increasing concentrations of palmitate (PA100–500 µM) or fructose (F100–500 µM) for 24 hours. (C) Quantification of myotube diameter after PA treatment. (D) Quantification of myotube diameter after fructose treatment.

To further substantiate the atrophic effects observed morphologically, we assessed the expression of myosin heavy chain (MyHC) in C2C12 myotubes. MyHC is one of the most abundant contractile proteins in skeletal muscle and plays a central role in generating force during muscle contraction.

Consistent with the reduction observed in myotube diameter, Western blot analysis revealed a decrease in MyHC expression following palmitate treatment. Myotubes exposed to increasing concentrations of palmitate displayed a slight reduction in MyHC protein levels compared with control conditions, as shown by the representative protein bands and the corresponding quantification (Figure 11A and 11B).

A similar trend was observed following fructose treatment. In particular, MyHC expression progressively decreased with increasing fructose concentrations. Although the reduction observed at 100 µM was not statistically significant, a more pronounced decrease was detected at 500 µM, as shown by the protein bands in Figure 11C and the corresponding quantification in Figure 11D.

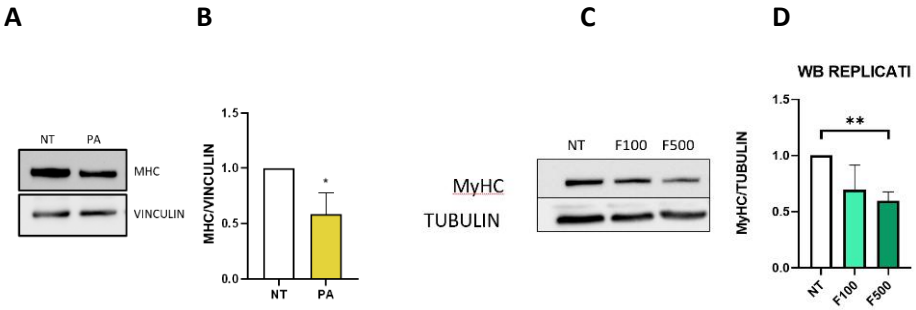

Figure 11. MHC reduction upon palmitate and fructose treatments. (A-D) Western blot analysis shows a reduction in MyHC protein levels in C2C12 myotubes treated with palmitate (PA500 µM) and with fructose (F100 µM and F500 µM) compared with NT. MyHC intensity was normalized to **vinculin** for palmitate-treated samples and to tubulin for fructose-treated samples. Data are presented as mean ± standard error of the mean (SEM). Statistical analysis was performed using Student's *t*-test and ANOVA. $P < 0.01$ vs NT.

To better understand the interaction between lipid and sugar excess, an additional condition combining palmitate and fructose (PA500 + F500) was included. As illustrated in panel E, the combined treatment elicited an atrophic response comparable to that observed with either treatment alone, suggesting that the synergistic effect of them did not augment the reduction of myotube width.

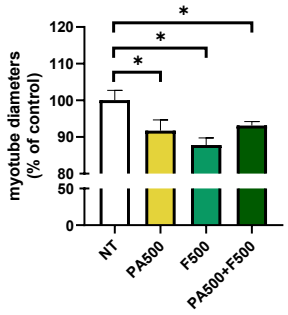

Figure 12. Comparison of NT, PA500 µM, F500 µM, and combined PA500 + F500 treatment, showing an enhanced reduction in myotube diameter under the combined condition. Data are presented as mean ± S.E.M. from at least three independent experiments. Statistical analysis was performed using one-way ANOVA. *p < 0.05, **p < 0.01 vs. NT.

As we moved for the *ex vivo* experiments**,** we then qualitatively assess lipid droplet (LD) accumulation under different metabolic stress conditions. C2C12 myotubes were stained with bodipy following 24-hour exposure to palmitate (PA500 µM), fructose (F500 µM), or their combined treatment (PA500 + F500). Interestingly, fluorescent imaging revealed distinct differences in intracellular LD distribution across conditions.

Untreated myotubes (NT) displayed minimal bodipy+ puncta, indicating a normal lipid profile with limited LD content (FIG 13A). In contrast, PA-treated cells exhibited a clear increase in LD accumulation, characterized by numerous bright green puncta distributed throughout the myotubes, consistent with palmitate-induced lipotoxicity (FIG 13A). Parallelly, fructose-treated myotubes also showed increased LD deposition compared to NT, although the intensity and density of BODIPY-positive structures appeared lower than in PA-treated cells. Notably, the combined PA+F500 treatment resulted in the most pronounced accumulation, with dense clusters of enlarged LDs visibly distributed along the length of the myotubes, suggesting a synergistic effect of fatty acid and fructose exposure. Overall, these qualitative observations align with the quantitative LD area analysis, confirming that both palmitate and fructose promote lipid storage in skeletal muscle cells, with the combined treatment exerting the strongest lipogenic effect.

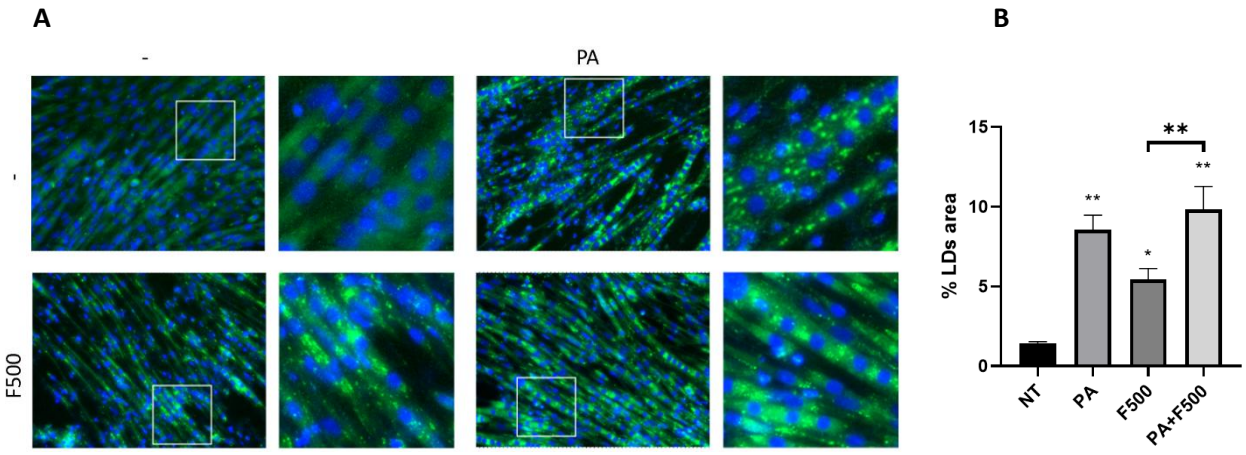

Figure 13. Palmitate and fructose treatments increase lipid droplet accumulation in C2C12 myotubes. (A) Representative BODIPY (green) and DAPI (blue) fluorescence images of myotubes following 24-hour exposure to PA500 µM, F500 µM, or their combination (PA500 + F500). Palmitate and

fructose both increase LD formation compared to untreated cells, with the combined treatment producing the strongest accumulation. (B) Quantification of lipid droplet area expressed as percentage of total myotube area. All treatments significantly increase LD accumulation compared to NT, with PA + F500 showing the highest LD content. Data are presented as mean ± SEM. *p < 0.05, **p < 0.01 vs NT; *$p < 0.01$ *between indicated groups.*

Discussion

The present study was designed to investigate the impact of chronic high-fat diet (HFD), alone or combined with fructose supplementation (HFD+F), on skeletal muscle homeostasis, including weight, morphology, atrophic signaling, and lipid accumulation, using both *in vivo* and *in vitro* approaches. Despite in literature the role of high-fat diet and fructose is more often associated in the onset of obesity (21,30), its role in skeletal muscle and sarcopenic obesity (SO) is until now not well deciphered, thus, we employed both *in vivo* model to dissect the effect of a high-fat high-fructose diet on skeletal muscle and the *in vitro* one to better understand the mechanisms underlying early stages of SO.

Our *in vivo* findings demonstrate that prolonged exposure to HFD, with or without fructose supplementation, induces a robust increase in body weight and white adipose tissue mass, confirming the effectiveness of the dietary protocol in promoting obesity. Both epididymal and subcutaneous fat depots were significantly enlarged in HFD and HFD+F groups compared with normal diet controls (ND), whereas brown adipose tissue was not significantly affected. These results are consistent with previous reports showing that high-fat feeding preferentially expands white adipose depots and promotes systemic metabolic dysfunction (21). Interestingly, fructose supplementation did not further increase white fat accumulation beyond that induced by HFD alone, suggesting that, in the context of an already lipid-rich diet, fructose does not substantially amplify peripheral fat storage. However, fructose exerted organ-specific effects, as evidenced by increased spleen and liver weights in the HFD+F group. The enlargement of the spleen may reflect heightened systemic inflammation, while the increase in liver weight is compatible with enhanced hepatic lipid accumulation and early steatotic changes, in agreement with studies demonstrating fructose-driven *de novo* lipogenesis and hepatic triglyceride synthesis (24,29,31). Although future studies will be focused on spleen and liver to unravel systemic inflammation and homeostasis, our project aim was to investigate the role of high-fat and fructose in skeletal muscle.

Despite the marked increase in total body mass and adiposity, skeletal muscle weight remained unchanged across dietary groups. Gastrocnemius, tibialis anterior, and quadriceps muscles did not exhibit significant differences in mass, indicating that overt muscle wasting did not occur under our experimental conditions (FIG 4). This observation suggests that, at least at the gross anatomical level, chronic HFD with or without fructose does not immediately induce measurable muscle mass loss at the timepoint used for our experimental plan. However, SO is characterized not only by reduced muscle mass but also by impaired muscle quality. Therefore, preservation of muscle weight does not necessarily imply preserved muscle health or function, since several mechanisms could be implicated in deregulating its metabolism.

Indeed, histological analysis revealed a striking increase in intramuscular lipid droplets in HFD and HFD+F mice, as demonstrated by bodipy staining. The percentage of lipid-positive fibers was significantly elevated in both diet-treated groups compared with controls, while no additional increase was observed in the HFD+F group relative to HFD alone. These data indicate that high-fat feeding is sufficient to promote substantial intramyocellular lipid accumulation, and fructose does not further exacerbate this parameter in vivo. Importantly, the general architecture of muscle fibers, as assessed by laminin staining and cross-sectional area (CSA) measurements, was preserved. Neither overall CSA nor the CSA of lipid-rich versus lipid-poor fibers differed among groups, supporting the conclusion that structural atrophy had not yet developed.

The coexistence of preserved muscle mass and fiber size with increased lipid infiltration suggests an early stage of metabolic remodeling rather than atrophy. Intramyocellular lipid accumulation has been strongly associated with insulin resistance and impaired mitochondrial function (32). As demonstrated by Samuel

and Shulman (2012) excess lipid droplets can generate bioactive lipid intermediates such as ceramides and diacylglycerols, which interfere with insulin signaling and activate stress pathways. Over time, such metabolic disturbances may predispose muscle to catabolic activation and functional decline. Therefore, our findings support the concept that intramuscular lipid deposition precedes measurable reductions in fiber size and may represent an early pathogenic event in diet-induced muscle dysfunction. For these reasons, the systemic effects observed in HFD+F mice, particularly increased liver and spleen weights, reinforce the notion that fructose may contributes to organ-specific metabolic bypassing key glycolytic regulatory steps and driving hepatic lipogenesis, leading to triglyceride accumulation and increased very low-density lipoprotein secretion. We speculate that dyslipidemia may indirectly affect skeletal muscle by increasing circulating fatty acid flux (33,34).

To strengthen the *in vivo* findings, we used differentiated C2C12 myotubes to examine the direct effects of palmitate, one of the most abundant and common circulating saturated fatty acid upon high-fat diet consumption (35), and fructose on skeletal muscle cells. In contrast to the absence of atrophy *in vivo*, both palmitate and fructose induced a dose-dependent reduction in myotube diameter *in vitro*. The most pronounced effects were observed at 500 µM for both treatments. These morphological changes were accompanied by decreased myosin heavy chain (MyHC) expression, particularly in fructose-treated cells at higher concentration. MyHC is a key contractile protein and a reliable marker of muscle differentiation and integrity; thus, its reduction supports the presence of atrophic remodeling at the cellular level.

Interestingly, the combined palmitate and fructose treatment confirm the atrophic effect, even if the synergic presence of them did not augment the outcome (Figure 12). Nevertheless, when lipid droplet accumulation was assessed, their co-presence elicited the most pronounced increase in intracellular lipid area, indicating additive effects on lipid storage.

These findings highlight a divergence between morphological atrophy and lipid deposition and the discrepancy between *in vivo* and *in vitro* atrophic outcomes deserves consideration. *In vivo*, multiple compensatory mechanisms may control the direct atrophic impact of nutrient excess. Moreover, the duration of exposure, although sufficient to induce obesity and lipid infiltration, may not have been long enough to trigger measurable reductions in fiber size. In contrast, cultured myotubes are directly exposed to defined concentrations of palmitate and fructose without systemic modulation, potentially amplifying stress responses. This controlled environment allows the detection of early molecular events that may precede structural atrophy in whole muscle.

The increase in lipid droplets observed both *in vivo* and *in vitro* supports the hypothesis that lipid overload is a central mediator of muscle metabolic dysfunction. Lipid droplets are dynamic organelles that normally buffer excess fatty acids and prevent lipotoxicity (13), however, chronic oversupply may overwhelm this protective system, leading to oxidative stress, mitochondrial impairment, and activation of proteolytic pathways such as the ubiquitin–proteasome system and autophagy–lysosome pathway (23). Although we did not directly measure atrogenes expression *in vivo*, the reduction in MyHC *in vitro* suggests that catabolic signaling may be engaged under nutrient stress.

In conclusion, chronic high-fat feeding induces obesity and significant intramuscular lipid accumulation without immediate reductions in muscle mass or fiber size, representing an early stage of muscle metabolic impairment. Fructose supplementation exacerbates systemic organ alterations, particularly in liver and spleen, and directly promotes atrophic and lipogenic responses in muscle cells *in vitro*. Together, these findings, despite need some further experiments, support the idea that the combination of lipid and

fructose may disrupt skeletal muscle homeostasis primarily through metabolic remodeling and lipid deposition before overt structural atrophy becomes evident, providing mechanistic insight into the early pathogenesis of SO.

Bibliography

1. Frontera WR, Ochala J. Skeletal Muscle: A Brief Review of Structure and Function. Calcif Tissue Int. 2015 Mar 1;96(3):183–95. doi:10.1007/s00223-014-9915-y

2. White HJ, Bordes SJ, Borger J. Anatomy, Abdomen and Pelvis: Aorta. In: StatPearls [Internet]. Treasure Island (FL): StatPearls Publishing; 2025 [cited 2025 Aug 7]. Available from: http://www.ncbi.nlm.nih.gov/books/NBK537319/ PubMed PMID: 30726004.

3. Yin L, Li N, Jia W, Wang N, Liang M, Yang X, et al. Skeletal muscle atrophy: From mechanisms to treatments. Pharmacol Res. 2021 Oct 1;172:105807. doi:10.1016/j.phrs.2021.105807

4. Sartori R, Romanello V, Sandri M. Mechanisms of muscle atrophy and hypertrophy: implications in health and disease. Nat Commun. 2021 Jan 12;12(1):330. doi:10.1038/s41467-020-20123-1

5. Ziaaldini MM, Marzetti E, Picca A, Murlasits Z. Biochemical Pathways of Sarcopenia and Their Modulation by Physical Exercise: A Narrative Review. Front Med. 2017 Oct 4;4:167. doi:10.3389/fmed.2017.00167 PubMed PMID: 29046874; PubMed Central PMCID: PMC5632757.

6. Schiaffino S, Dyar KA, Ciciliot S, Blaauw B, Sandri M. Mechanisms regulating skeletal muscle growth and atrophy. FEBS J. 2013 Sep;280(17):4294–314. doi:10.1111/febs.12253 PubMed PMID: 23517348.

7. Pang X, Zhang P, Chen X, Liu W. Ubiquitin-proteasome pathway in skeletal muscle atrophy. Front Physiol. 2023 Nov 17;14. doi:10.3389/fphys.2023.1289537

8. Zhang H, Qi G, Wang K, Yang J, Shen Y, Yang X, et al. Oxidative stress: Roles in skeletal muscle atrophy. Biochem Pharmacol. 2023 Aug 1;214:115664. doi:10.1016/j.bcp.2023.115664

9. Manivannan P, Reddy V, Mukherjee S, Clark KN, Malathi K. RNase L Induces Expression of A Novel Serine/Threonine Protein Kinase, DRAK1, to Promote Apoptosis. Int J Mol Sci. 2019 Jul 19;20(14). doi:10.3390/ijms20143535

10. Donini LM, Busetto L, Bischoff SC, Cederholm T, Ballesteros-Pomar MD, Batsis JA, et al. Definition and Diagnostic Criteria for Sarcopenic Obesity: ESPEN and EASO Consensus Statement. Obes Facts. 2022 Feb 23;15(3):321–35. doi:10.1159/000521241 PubMed PMID: 35196654; PubMed Central PMCID: PMC9210010.

11. Wannamethee SG, Atkins JL. Muscle loss and obesity: the health implications of sarcopenia and sarcopenic obesity. Proc Nutr Soc. 2015 Nov;74(4):405–12. doi:10.1017/S002966511500169X

12. Donini LM, Busetto L, Bischoff SC, Cederholm T, Ballesteros-Pomar MD, Batsis JA, et al. Definition and diagnostic criteria for sarcopenic obesity: ESPEN and EASO consensus statement. Clin Nutr. 2022 Apr 1;41(4):990–1000. doi:10.1016/j.clnu.2021.11.014 PubMed PMID: 35227529.

13. Bosma M. Lipid droplet dynamics in skeletal muscle. Exp Cell Res. 2016 Jan 15;340(2):180–6. doi:10.1016/j.yexcr.2015.10.023 PubMed PMID: 26515552.

14. Neeland IJ, Poirier P, Després JP. Cardiovascular and Metabolic Heterogeneity of Obesity. Circulation. 2018 Mar 27;137(13):1391–406. doi:10.1161/CIRCULATIONAHA.117.029617

15. Batsis JA, Villareal DT. Sarcopenic obesity in older adults: aetiology, epidemiology and treatment strategies. Nat Rev Endocrinol. 2018 Sep;14(9):513–37. doi:10.1038/s41574-018-0062-9 PubMed PMID: 30065268; PubMed Central PMCID: PMC6241236.

16. Polyzos SA, Margioris AN. Sarcopenic obesity. Hormones. 2018 Sep 1;17(3):321–31. doi:10.1007/s42000-018-0049-x

17. Buettner R, Schölmerich J, Bollheimer LC. High-fat Diets: Modeling the Metabolic Disorders of Human Obesity in Rodents. Obesity. 2007;15(4):798–808. doi:10.1038/oby.2007.608

18. Lee H, Lee IS, Choue R. Obesity, Inflammation and Diet. Pediatr Gastroenterol Hepatol Nutr. 2013 Sep 1;16(3):143–52. doi:10.5223/pghn.2013.16.3.143

19. Jia Z, Wang Z, Pan H, Zhang J, Wang Q, Zhou C, et al. Crosstalk between fat tissue and muscle, brain, liver, and heart in obesity: cellular and molecular perspectives. Eur J Med Res. 2024 Dec 31;29(1):637. doi:10.1186/s40001-024-02176-w

20. Hill JO, Melanson EL. Overview of the determinants of overweight and obesity: current evidence and research issues. Med Sci Sports Exerc. 1999 Nov;31(11 Suppl):S515-521. doi:10.1097/00005768-199911001-00005 PubMed PMID: 10593521.

21. Hariri N, Thibault L. High-fat diet-induced obesity in animal models. Nutr Res Rev. 2010 Dec;23(2):270–99. doi:10.1017/S0954422410000168 PubMed PMID: 20977819.

22. High Fat Diet - an overview | ScienceDirect Topics [Internet]. [cited 2026 Mar 1]. Available from: https://www.sciencedirect.com/topics/agricultural-and-biological-sciences/high-fat-diet

23. Yuzefovych LV, Musiyenko SI, Wilson GL, Rachek LI. Mitochondrial DNA Damage and Dysfunction, and Oxidative Stress Are Associated with Endoplasmic Reticulum Stress, Protein Degradation and Apoptosis in High Fat Diet-Induced Insulin Resistance Mice. PLOS ONE. 2013 Jan 16;8(1):e54059. doi:10.1371/journal.pone.0054059

24. Tappy L, Lê KA. Metabolic Effects of Fructose and the Worldwide Increase in Obesity. Physiol Rev. 2010 Jan;90(1):23–46. doi:10.1152/physrev.00019.2009

25. Bray GA, Popkin BM. Dietary Sugar and Body Weight: Have We Reached a Crisis in the Epidemic of Obesity and Diabetes? Diabetes Care. 2014 Apr;37(4):950–6. doi:10.2337/dc13-2085 PubMed PMID: 24652725; PubMed Central PMCID: PMC9514031.

26. Stanhope KL. Sugar consumption, metabolic disease and obesity: The state of the controversy. Crit Rev Clin Lab Sci. 2016 Feb;53(1):52–67. doi:10.3109/10408363.2015.1084990 PubMed PMID: 26376619; PubMed Central PMCID: PMC4822166.

27. Portal de Periódicos da CAPES [Internet]. [cited 2025 Aug 20]. Fructose, uricase, and the Back-to-Africa hypothesis. Available from: https://www.periodicos.capes.gov.br/index.php/acervo/buscador.html?task=detalhes&id=W2142563790

28. Crescenzo R, Bianco F, Falcone I, Coppola P, Liverini G, Iossa S. Increased hepatic de novo lipogenesis and mitochondrial efficiency in a model of obesity induced by diets rich in fructose. Eur J Nutr. 2013 Mar 1;52(2):537–45. doi:10.1007/s00394-012-0356-y

29. Softic S, Cohen DE, Kahn CR. Role of Dietary Fructose and Hepatic de novo Lipogenesis in Fatty Liver Disease. Dig Dis Sci. 2016 May;61(5):1282–93. doi:10.1007/s10620-016-4054-0 PubMed PMID: 26856717; PubMed Central PMCID: PMC4838515.

30. Li Z, Fan X, Gao F, Pan S, Ma X, Cheng H, et al. Fructose metabolism and its roles in metabolic diseases, inflammatory diseases, and cancer. Mol Biomed. 2025 Jun 23;6(1):43. doi:10.1186/s43556-025-00287-2

31. Softic S, Gupta MK, Wang GX, Fujisaka S, O'Neill BT, Rao TN, et al. Divergent effects of glucose and fructose on hepatic lipogenesis and insulin signaling. J Clin Invest. 2017 Nov 1;127(11):4059–74. doi:10.1172/JCI94585 PubMed PMID: 28972537; PubMed Central PMCID: PMC5663363.

32. Kakehi S, Tamura Y, Takeno K, Sakurai Y, Kawaguchi M, Watanabe T, et al. Increased intramyocellular lipid/impaired insulin sensitivity is associated with altered lipid metabolic genes in muscle of high responders to a high-fat diet. Am J Physiol-Endocrinol Metab. 2016 Jan;310(1):E32–40. doi:10.1152/ajpendo.00220.2015

33. Samuel VT, Shulman GI. Integrating Mechanisms for Insulin Resistance: Common Threads and Missing Links. Cell. 2012 Mar 2;148(5):852–71. doi:10.1016/j.cell.2012.02.017 PubMed PMID: 22385956; PubMed Central PMCID: PMC3294420.

34. Metabolic Effects of Fructose and the Worldwide Increase in Obesity | Physiological Reviews | American Physiological Society [Internet]. [cited 2026 Mar 12]. Available from: https://journals.physiology.org/doi/full/10.1152/physrev.00019.2009?rfr_dat=cr_pub++0pubmed&url_ver=Z39.88-2003&rfr_id=ori%3Arid%3Acrossref.org

35. de Hart NMMP, Petrocelli JJ, Nicholson RJ, Yee EM, Ferrara PJ, Bastian ED, et al. Palmitate-Induced Inflammation and Myotube Atrophy in C2C12 Cells Are Prevented by the Whey Bioactive Peptide, Glycomacropeptide. J Nutr. 2023 Oct;153(10):2915–28. doi:10.1016/j.tjnut.2023.08.033 PubMed PMID: 37652286; PubMed Central PMCID: PMC10731921.